

Purdue University

Purdue e-Pubs

International High Performance Buildings
Conference

School of Mechanical Engineering

2022

Assessment Of Short-Term Aquifer Thermal Energy Storage For Energy Management In Greenhouse Horticulture: Modeling And Optimization

Queralt Altes-Buch

Tanguy Robert

Sylvain Quoilin

Vincent Lemort

Follow this and additional works at: <https://docs.lib.purdue.edu/ihpbc>

Altes-Buch, Queralt; Robert, Tanguy; Quoilin, Sylvain; and Lemort, Vincent, "Assessment Of Short-Term Aquifer Thermal Energy Storage For Energy Management In Greenhouse Horticulture: Modeling And Optimization" (2022). *International High Performance Buildings Conference*. Paper 429.
<https://docs.lib.purdue.edu/ihpbc/429>

This document has been made available through Purdue e-Pubs, a service of the Purdue University Libraries.
Please contact epubs@purdue.edu for additional information.

Complete proceedings may be acquired in print and on CD-ROM directly from the Ray W. Herrick Laboratories at
<https://engineering.purdue.edu/Herrick/Events/orderlit.html>

Assessment of short-term aquifer thermal energy storage for energy management in greenhouse horticulture: modeling and optimization

Queralt ALTES-BUCH^{1*}, Tanguy ROBERT², Sylvain QUOILIN¹, Vincent LEMORT¹

¹ Energy Systems Research Unit, Faculty of Applied Sciences, University of Liege,
Liege, Belgium

{qaltes, squoilin, vincent.lemort}@uliege.be

² Urban and Environmental Engineering Research Unit, Faculty of Applied Sciences, University
of Liege, Liege, Belgium
tanguy.robert@uliege.be

* Corresponding Author

ABSTRACT

In this work, the use of the thermal energy storage in alluvial aquifers is proposed as a sustainable solution for supplying the energy demand of greenhouses. Air-conditioning greenhouses during summer allows for storing their energy surplus in an underground seasonal buffer that can be used, in winter, for heating via a heat pump. The evaluation of the benefits arising from using aquifer thermal energy storage (ATES) for supplying the energy demand in greenhouse applications requires the modeling of a greenhouse climate model, heating distribution systems (i.e., heating pipes and coils), a heat pump and the ATES system. The models are sized to a case study, which is based on a 100 m thick aquifer in the Cretaceous chalk located in Wallonia (Belgium), and are simulated for two years. The first year is only devoted to storage and emulates the creation of the cold and warm wells. In the second year, the thermal energy stored in the aquifer is recovered according to the needs of the greenhouse (the cold well is used during air-conditioning and the warm well during heating). Results show that shallow alluvial aquifers can be very valuable and can provide a sustainable solution when heating and cooling greenhouses. However, the greenhouse climate controller must be correctly calibrated in order to maintain a balanced ATES system. More specifically, greenhouses in the latitude of Belgium are forced to increase their cooling consumption, which is possible thanks to the flexibility offered by greenhouses. Otherwise, the system may not be sustainable due to the higher needs of heating.

1. INTRODUCTION

Glass greenhouses are a well established technology used to cultivate crops. By heating and increasing the exposure to light via lamps, they allow colder regions for cultivating breeds of flowers and vegetables that naturally grow in temperate or tropical climates. One of the many benefits of technologically equipped greenhouses is the potential they offer for optimizing crop production. On the one hand, the focus on climate control has enabled maximizing crop production both quantitatively and qualitatively. The latter has lead countries such as the Netherlands to be the largest exporter of tomatoes in Europe, even above Spain (Commission, 2021). On the other hand, climate control comes at a high energy cost. To maintain the optimal temperature, light and CO₂ levels that maximize the crop yield, greenhouses may consume (prohibitively) substantial amounts of energy for heating, electricity, CO₂ and cooling.

Even in the Atlantic and Central European regions, cooling is needed because greenhouses have a surplus of thermal energy in summer that must be removed to avoid yield reduction and crop diseases (Stanghellini, Ooster, and Heuvelink, 2018). The most established cooling method in these regions is natural ventilation. However, when ventilating the thermal energy surplus is lost to the environment. In addition, if the target temperature is lower than the outside (dry or wetbulb) temperature, non-passive cooling is required. Most of the existing mechanical cooling methods for greenhouses have been developed for hot, dry climate regions whose primary energy consumption is cooling. Based on evaporative cooling, these systems are

not suited to the Atlantic and Central European climates. With an increased need for active cooling during summer in regions with mainly heating requirements, sustainable technologies that allow for seasonal energy recovery in greenhouses have become a relevant scope of research.

In a greenhouse with reduced ventilation, active cooling in summer allows for storing the thermal energy surplus in an underground seasonal buffer that can later be used for heating in winter (Stanghellini, Ooster, and Heuvelink, 2018). Among the available underground storage technologies, aquifer thermal energy storage (ATES) is the most suitable for that purpose. The high percentage of heat recovery makes ATES useful for demand-side management applications such as greenhouses (De Schepper et al., 2019).

The main goal of this work is to assess the energy recovery potential of greenhouses with thermal energy storage in shallow alluvial aquifers in the Atlantic climate. To that end, this work models and simulates a case study based on a greenhouse coupled to a 100 m thick synthetic chalk aquifer mimicking a real Cretaceous chalk aquifer in the Mons area in Wallonia (Belgium). The aquifer is characterized by a slow ambient groundwater flow. The flows are at 10-15°C for heating and at 5-10°C for cooling. While heating requires the use of a heat pump, cooling is possible directly at the aquifer temperature. The greenhouse is used for growing tomato crop and is equipped with lighting and a CO₂ enrichment system. The aquifer is assumed to supply the thermal demand at all times.

The greenhouse and the thermal distribution and generation systems are modeled by means of the Greenhouses Library (Altes-Buch, Quoilin, and Lemort, 2019), an open-source Modelica library for the dynamic simulation of greenhouse climate and energy systems. The Greenhouses library also provides control strategies for the heating, ventilation and other appliances (e.g. CO₂ enrichment and lighting), which determine the combined demand of the greenhouse during the simulation period. The aquifer is modeled by a deterministic 3D ground water flow and heat transport numerical model in the presented case study.

The case study is simulated for a period of two years. Results show that shallow alluvial aquifers can be very valuable and can provide a sustainable solution when heating and cooling greenhouses. However, to achieve so, the greenhouse climate controller must be correctly calibrated. In fact, to maintain a balanced system, greenhouses in the latitude of Belgium are forced to increase their cooling consumption. Otherwise, the system is imbalanced due to the higher needs of heating.

2. MODELING

The evaluation of the benefits arising from using ATES for supplying the energy demand in greenhouse applications requires to model several thermal systems, namely: a greenhouse climate model, heating distribution systems (i.e. heating pipes, heating and cooling coils), generation systems (i.e. heat pump) as well as the ATES system.

2.1 Greenhouse climate

Greenhouse climate models are useful to quantify the energy performance and the crop production given a greenhouse design, outdoor climate and a specific control. Similar to building energy modeling, greenhouse climate models compute the indoor climate of a greenhouse by describing the flows between its components and solving their respective energy balances. Since in greenhouses the indoor climate is described by three variables (i.e. the temperature, the humidity and the CO₂ concentration in the air), the greenhouse model also includes moisture and CO₂ mass balances on the air.

The sensible energy balances are written in the form of Equation (1) and are applied to all components of the greenhouse. As shown in Figure 1, the greenhouse model consists of the air, the canopy, the envelope (i.e. the cover and the floor), the heating pipes and the thermal screen. The thermal screen is an horizontally movable membrane used to reduce the far-infrared radiative losses to the cover and to the sky. When the screen is deployed, the air of the greenhouse is divided in two zones, i.e. below and above the screen. These zones are modeled separately and their respective climate is assumed to be homogeneous (Altes-Buch, Quoilin, and Lemort, 2022).

$$\rho c_p V \frac{dT}{dt} = \sum \dot{Q} + \sum \dot{H}_{sens} \quad (1)$$

Apart from the energy flows exchanged within the forementioned greenhouse components, the model takes into account the moisture exchanged by natural ventilation with the outside air, the condensation at the cover and thermal screen, as well as the transpiration and photosynthesis (CO_2 consumption) from the canopy.

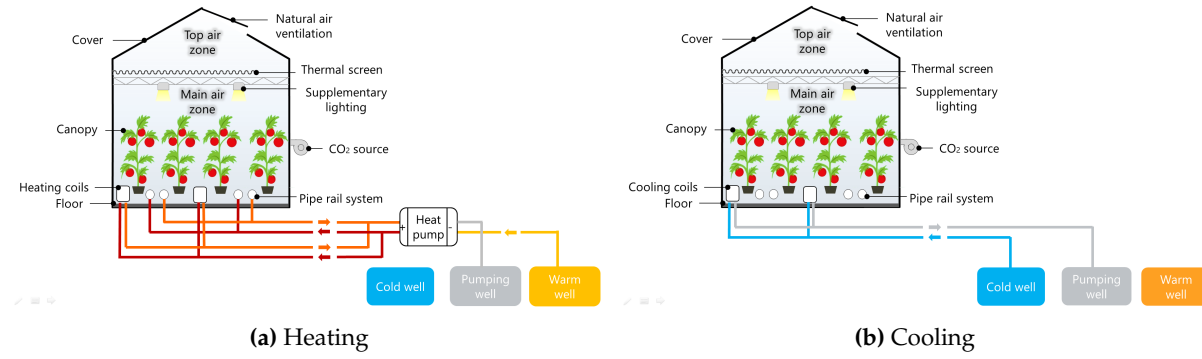


Figure 1: Sketch of the system

2.2 Heat distribution systems

In order to have an optimal thermal energy recovery, the thermal energy distribution systems inside the greenhouse must be selected by taking into account potential constraints from the supply source, such as the supply temperature, and from the crop (Urban and Urban, 2010). For instance, in order to keep crop yield at an optimal level, it has been proven that, the temperature of the canopy is of utmost importance, not the temperature of the air that surrounds it. To that end, radiative systems (e.g. water pipes) are preferred over purely convective systems, since not only they heat the air through convection, but also they heat the canopy through long-wave radiation. As an illustration, in (Altes-Buch, Quoilin, and Lemort, 2022) it is demonstrated that in winter the canopy absorbs as much radiative heat flow from the pipes than convective heat flow from the air.

In this work, water pipes are selected as the primary heating distribution system. Water pipes are the most established technology for distributing heat in regions with high heating requirements. They usually cover the entire greenhouse floor through parallel loops that go along the crop rows. Therefore, despite their high investment cost, they allow for an horizontal temperature distribution of the highest quality. In order to be used as transport rails for the harvest, they are plain pipes (i.e. without fins) placed some centimeters above the ground. The installed capacity (diameter and length) follows greenhouse crop rows setup standards. Depending on the heat generation system that supplies them, they work between 45°C and 90°C .

Contrary to the case of heating, radiative systems are less adequate for cooling greenhouses. The plain nature of the water pipes implies a low heat transfer coefficient to the air. For the given aquifer supply temperature and the standard piping installed capacity (restricted to increase due to the crops setup), the water pipes are not able to meet the peak cooling demand. Additionally, the radiative exchange decreases the canopy temperature below the optimal range, which implies substantial yield reduction. It is therefore not desirable to lower supply temperature by means of a chiller to meet the peak demand. In order to be able to meet the peak demand without production losses, purely convective systems are a preference. Out of the available convective distribution systems, only water-to-air units are suitable for ATES applications. This work proposes the use of coils.

Given that the standard installed piping capacity is insufficient to supply the peak heating demand in winter (cfc Section 3.3), the coils are also used for heating distribution. They are used during peak heating demand hours as an accessory to the pipe system. This combination allows maintaining the canopy temperature at an optimal level both when heating and cooling to avoid yield reduction.

2.2.1 Heating pipes

The pipes heat the greenhouse air through hindered convection, but also the canopy, the floor and the

greenhouse cover through long-wave radiation. Because of their length, a constant heat transfer coefficient cannot be assumed along the pipe. As a consequence, the heating pipes are modeled using a finite volume approach by means of a discretized model that divides the pipes into several cells, each one connected in series by a node (Quoilin et al., 2014). In each cell, the flow is described with enthalpy as a state variable. The dynamic energy balance and static mass and momentum balances are applied in each cell. The model assumes uniform speed through the cross section as well as constant pressure. Axial thermal energy transfer is neglected. The heat flow is computed by an ideal heat transfer model with constant heat transfer coefficient. The energy balance on the fluid for a cell i is described by:

$$V_i \rho_i \frac{dh_i}{dt} + \dot{M}(h_{ex,i} - h_{su,i}) = A_i \dot{q}_i, \quad i = 1, 2, \dots, N_{cell} \quad (2)$$

where h_i is the fluid specific enthalpy at cell i , and h_{ex} and h_{su} are the enthalpy at the cell's outlet and inlet nodes, respectively.

2.2.2 Heating and cooling coils

Coils can work in dry, partially wet or wet regimes. In most cases, cooling and drying are done simultaneously with the coil working in a wet regime. In a partially wet regime, condensation appears in a point where the contact temperature is lower than the dew point temperature of the air. In this case, a part of the coil works in dry regime, while the rest works in a wet regime.

Over the past decades, water cooling coil models have been the subject of a substantial literature. Many models using different approaches have been developed and validated, the most common ones being:

- Single zone epsilon-NTU models (Lebrun et al., 1990; Morisot, Marchio, and Stabat, 2002),
- Variable boundary models (Brandemuehl, 1993), and
- Finite elements (Gang, Mingsheng, and Claridge, 2007) and lumped models.

In this work, the model proposed in Lebrun et al., 1990 is implemented because of its increased robustness for similar levels of accuracy in comparison to the rest of the models, as reviewed in Gendebien, Bertagnolio, and Lemort, 2010. The model is characterized by three main hypothesis. The first one is that it assumes the cooling coil either completely dry or completely wet. In reality, both options underestimate the heat transfer rate. On the one hand, if the coil is assumed completely dry, the latent heat transfer is neglected. On the other hand, if the coil is assumed completely wet, the model predicts air moisture in the dry part of the coil, which means it considers a negative latent heat transfer rate. Given that both descriptions underestimate the total exchange, the model sets the cooling power to the one with the highest exchanged power:

$$\dot{Q}_{ccoil} = \max(\dot{Q}_{dry}, \dot{Q}_{wet}) \quad (3)$$

The heating coil is modeled in a simpler manner since only the dry regime must be described.

The second hypothesis states that in the energy balance in wet regime (which takes into account the latent heat), the air can be substituted by a fictitious fluid the enthalpy of which is completely defined by the wet temperature of the fluid. Therefore, the energy balance described by Equation (4) is equivalent to Equation (5).

$$\dot{Q}_{wet} = \dot{M}_{air} \cdot (h_{air,su} - h_{air,ex,wet}) - \dot{M}_{air} \cdot (w_{air,su} - w_{air,ex,wet}) \cdot c_w \cdot T_{air,ex,wet} \quad (4)$$

$$\dot{Q}_{wet} = \dot{M}_{air} \cdot c_{p,airf} \cdot (T_{wb,su} - T_{wb,ex,wet}) \quad (5)$$

Finally, in order to compute the state in which the air exits the coil, the model defines a semi-isothermal exchanger that takes the air as one fluid and the external surface of the coil as the other, as described by:

$$h_{air,su} - h_{air,ex,wet} = \varepsilon_{c,wet} \cdot (h_{air,su} - h_{c,wet}) \quad (6)$$

$$w_{air,su} - w_{air,ex,wet} = \varepsilon_{c,wet} \cdot (w_{air,su} - w_{c,wet}) \quad (7)$$

$$\varepsilon_{c,wet} = 1 - \exp(-NTU_{c,wet}) \quad (8)$$

$$NTU_{c,wet} = \frac{1}{R_{air} \cdot \dot{C}_{air}} \quad (9)$$

2.3 Water-to-water heat pump

The heat pump model implemented in this work predicts the performance at both full- and partial-load operation for different working conditions by means of three polynomial laws fitted through manufacturing data (Bolther et al., 1999). The first law describes the coefficient of performance (COP) at full load as a function of the temperatures at the evaporator inlet and at the condenser outlet:

$$EIRFT = \frac{COP_n}{COP_{fl}} = \alpha_0 + \alpha_1 \cdot \Delta T + \alpha_2 \cdot \Delta T^2 \quad (10)$$

where

$$\Delta T = \frac{T_{su,ev}}{T_{ex,cd}} - \frac{T_{su,ev,n}}{T_{ex,cd,n}} \quad (11)$$

with the temperatures values being in Kelvins.

The second law describes the heating power at full load as a function of the temperatures at the evaporator inlet and at the condenser outlet:

$$CAPFT = \frac{\dot{Q}_{cd,fl}}{\dot{Q}_{cd,n}} = \beta_0 + \beta_1 \cdot (T_{su,ev} - T_{su,ev,n}) + \beta_2 \cdot (T_{ex,cd} - T_{ex,cd,n}) \quad (12)$$

Finally, the third law describes the performance at partial load:

$$EIRFPLR = \frac{\dot{W}_{pl}}{\dot{W}_{fl}} = \delta_0 + \delta_1 \cdot PLR_{cd} + \delta_2 \cdot PLR_{cd}^2 \quad (13)$$

where the part load ratio is described by:

$$PLR_{cd} = \frac{\dot{Q}_{cd,pl}}{\dot{Q}_{cd,fl}} \quad (14)$$

and the electrical power required at the compressor at full load operation is described by:

$$\dot{W}_{fl} = \frac{\dot{Q}_{cd,fl}}{COP_{fl}} \quad (15)$$

2.4 Aquifer Thermal Energy Storage

The synthetic model used to simulate groundwater flow and heat transport represents a 100 m thick aquifer typical of the Cretaceous chalk area located in Mons, in Belgium. These aquifers are very productive and are good targets for ATES systems. As an example, pumping rates can reach up to 300 m³/h. This model was built with the MODFLOW (Harbaugh et al., 2000) and MT3DMS (Zheng and Wang, 1999) suites. For the latter code simulating only solute transport, we took advantage of the analogy between the equations of heat transport and solute transport, as previously shown and validated in Hecht-Méndez et al., 2010.

The modeled ATES system consists of three wells, the so-called triplet. The first well (the pumping well) always supplies water at 10°C. The other two wells are used to store (1) cold water (at about 5°C) when

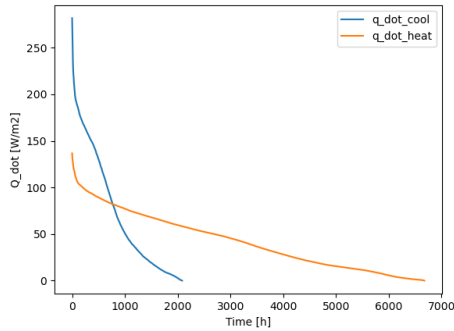


Figure 2: Yearly load duration curves of cooling and heating

the greenhouse is heated and (2) hot water (at about 15°C) when the greenhouse is air-conditioned. These two wells are called the cold well and the warm well respectively. The inputs of the model depend on the direction of pumping. When pumping from the pumping well, the inputs are the pumping rate in the pumping well and the injection rates at the cold and warm well with their associated temperatures. When pumping from the warm and cold wells, the input is still the pumping rates at the different wells (which are defined by the greenhouse demand). However, the water temperature of the pumped water from the cold and warm wells is now an output of the model.

The hydraulic conductivity is the main parameter for groundwater flow simulation. The hydraulic conductivity is set to 10^{-4} m s^{-1} , which is a mean value for this kind of aquifer. As for the thermal parameters that do not vary in great proportion in aquifers, we took the same parameters that can be found in Hecht-Méndez et al., 2010.

The ATES system was designed according to Dutch best practice. This means for example that the distance between the different wells is sufficiently large to avoid any thermal interaction between the thermal plumes stored in the aquifer (Bloemendaal, Olsthoorn, and Boons, 2014; Bloemendaal, Jaxa-Rozen, and Olsthoorn, 2018).

3. SIZING OF THE COMPONENTS

The simulation of the case study requires the sizing of the modeled components. This section summarizes the sizing of all of the models presented in Section 2.

3.1 Greenhouse sizing

The greenhouse is sized to the geological site. The alluvial plain from this case study allows for a construction of a 1 ha greenhouse. In order to size the greenhouse energy systems, the greenhouse model described in Section 2.1 has been simulated for a period of one year. The goal is to obtain the peak heating and cooling powers required by the greenhouse. The climate set-points are computed as proposed in Altes-Buch and Lemort, 2018 and are suited to the crop needs. The obtained yearly load duration curves for heating and cooling are shown in Figure 2.

Results show that energy for heating purposes is demanded about three quarters of the year, with a peak demand of 137 W m^{-2} . Cooling is required only in summer and has a higher peak demand at 278 W m^{-2} . This is, as expected, due to the greenhouse effect on sunny warm summer days.

3.2 Heating pipes sizing

As previously mentioned, water pipes are placed along the crop rows to keep a homogeneous climate on an horizontal axis and to serve as rails for harvest transport. The installed capacity of the pipes is therefore defined by the setup of the crop rows over the greenhouse floor area. In a classic Venlo type greenhouse, crop rows are separated by 1.6 m (De Zwart, 1996). Therefore, the required installed capacity for a greenhouse of 1 ha, assuming 200 m over 50 m, is 125 loops of 100 m.

Given the considerable length of each pipe loop, two conditions must be respected in order to have a homogeneous climate on an horizontal axis. First, the power output is adjusted by temperature control. The mass flow rate is therefore constant to the nominal value. Second, small temperature differences from the supply to the exhaust are desired. Typical controls aim for a temperature difference of about 5 to 7 degrees.

Assuming a loop completion time of 20 min (De Zwart, 1996) and a standard pipe diameter of 51 mm (Urban and Urban, 2010), the nominal mass flow rate is computed to be 0.14 kg s^{-1} . Considering a 6 degrees temperature difference supply-exhaust, the maximum power output of the pipes is around 46 W m^{-2} , which is 42% of the peak demand (assuming the peak at 110 W m^{-2} instead of 137 W m^{-2} , given the low frequency of the points above 110 W m^{-2}). As a reminder, the rest of the heat is supplied by the coils.

3.3 Coils sizing

The coils are used for both heating and cooling. Given that the cooling demand is higher than the heating demand, the coils have been sized for cooling. When observing the steepness of the load duration curve, one may conclude that it is not cost-efficient to size the system according to the peak demand. Indeed, demand values above 200 W m^{-2} are only required few hours per year. However, the installed capacity must be high enough to allow for maintaining the air temperature below a certain threshold defined by the crop. The main reason is that the crop has temperature and humidity thresholds that, if exceeded, lead to crop yield reduction and potentially to crop diseases. For instance, many diseases are favored by temperatures between 24°C and 35°C (Urban and Urban, 2010). Additionally, the harvest rate at a maximum day temperature of 30°C , 35°C and 40°C is 91%, 79% and 52% of the one at 25°C (Vanthoor, 2011). In this work, the maximum acceptable air temperature has been established at 32°C . To comply with the later, the cooling coils must be able to supply 250 W m^{-2} . Given the characteristics of the modeled coils, the greenhouse must be equipped with 192 units (i.e. a share of 52 m^2 of greenhouse floor per unit).

As previously mentioned, coils are also used as an accessory to the heating pipes in case the heating demand is higher than the pipes installed capacity. Considering a heating peak demand of 110 W m^{-2} and the pipes maximum output of 46 W m^{-2} , the heating coils must be able to supply 64 W m^{-2} . Therefore, only a quarter of the installation (sized according to cooling needs) is required to provide the heating demand.

3.4 Heat pump sizing

Manufacturer data are necessary to fit the performance laws of the heat pump model. The heat pump must be able to provide the total heat demand, which is translated to a power of 1.13 MW at the condenser. The peak power can either be achieved by a single unit or by several smaller units working in parallel or series (e.g. 4 units of 283 kW). Manufacturer data that fits the size range useful for our case study could only be obtained for a water-to-water chiller. The characteristics at nominal load are displayed in Table 1. The coefficient of performance (COP) of a machine working in heat pump mode can be assumed as its energy efficiency ratio (EER) plus one:

$$\text{COP} = \text{EER} + 1 \quad (16)$$

Given the specifications and together with Equation (15), we compute an equivalent nominal heating power of 445 kW, which allows for supplying the peak demand by three units in parallel. The nominal cooling capacity and the power input are based on $\Delta T = 5\text{K}$ entering/leaving condenser water temperature. The chiller's working temperature range is:

- Evaporator outlet: from 4°C to 9°C , with 7°C as nominal operation.
- Condenser inlet: from 25°C to 45°C , with 30°C as nominal operation.

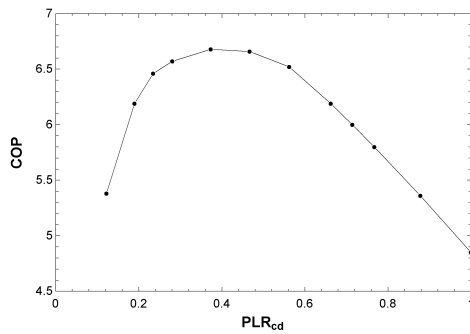
The chiller is a water-cooled machine equipped with 2 single-screw compressors and working with HFC-134a. Each compressor, integrated in 2 separate refrigerant circuits, can modulate continuously its capacity down to 25% by means of capacity slides, offering a cooling capacity reduction of the chiller down to 12.5%. Evaporator and condenser are shell-and-tube heat exchangers.

Equations (10) and (12) were fit with the data at full load operation and the working $\Delta T = 5\text{K}$. Equation (13) was fit with the data at part load operation (shown in Figure 3), which is given for a cooling power of

Table 1: Characteristics of chiller ECOPLUS XE - ST 100.2

Specifications	Values	Units
$\dot{Q}_{ev,n}$	366	kW
EER_n	4.62	-
$T_{ev,ex,n}$	7	°C
$T_{ev,su,n}$	12	°C
$T_{cd,su,n}$	30	°C
$T_{cd,ex,n}$	35	°C

324.2 kW and a compressor input of 84.3 kW. As it can be observed, the chiller performance are higher at part load operation, with a peak at 40% of load. The obtained calibration parameters are displayed in Table 2.

**Figure 3:** Performance at part load as a function of the part load ratio at the condenser**Table 2:** Coefficients of the heat pump model

Coefficient	Value
α_0	0.99777
α_1	-8.9186
α_2	39.826
β_0	1.00145
β_1	0.026347
β_2	-0.0026717
δ_0	0.0898214
δ_1	0.186482
δ_2	0.710761

3.5 ATES sizing

The ATES wells must be sized to the extraction volumes required by the greenhouse. These are the volumes needed at the heat pump evaporator and the cooling coils to provide the greenhouse demand. The volumes are computed by means of Simulation 1 in the experimental protocol. The simulation details are described in Section 4.1 and the results are later discussed in Section 5.

4. CASE STUDY

In order to quantify the energy recovery potential of the study site, the modeled system is simulated for two years:

- First year: the goal is to recover energy from the greenhouse and store it underground, thus forming a warm and a cold plume in the aquifer. To that end, the greenhouse demand for both heating and

cooling is provided by flows extracted from a pumping well at 10°C (i.e. the temperature of the site). The flows to the greenhouse are controlled such that the return temperature is $\pm 5\text{K}$ with respect to the supply temperature. The greenhouse heating and cooling returns are injected in two separate locations, the goal being to create a warm plume at 15°C around the warm well and inversely, a cold plume at 5°C around the cold well.

- Second year: the goal is to exploit the energy stored in the warm and cold wells as shown in Figure 1. To that end, the greenhouse demand flows are extracted from the warm and cold wells for heating and cooling (respectively). Both returns are injected to the pumping well.

Because of crop constraints, the start of the simulation must be equivalent to the start of the growing year. Since the studied crop is tomato, the simulation starts on December 10th, as proposed in Grisey and Brajeul, 2007. In the greenhouse model, a typical meteorological year of Brussels is used to represent the outdoor climate.

4.1 Experimental protocol

The overground models (i.e. the greenhouse climate model, the heat pump model, the water pipes model and the coils model) cannot be simulated simultaneously with the ATES model because they are based on two different simulation software. Therefore, the simulation of the global system requires iterations between the two platforms. To tackle the iteration process, the following experimental protocol is followed:

- **Simulation 1:** simulate the overground models over the first year

Goal: compute the greenhouse demand at the ATES level (i.e. the heat pump and coils flow rates and their return temperature)

To that end, the models have been interconnected as follows. The greenhouse climate model, in which the water pipes and coils models are integrated, is coupled to three heat pump models connected in parallel. The aggregated condensers' outlet/inlet are connected to the inlet/outlet of the water pipes and heating coils. The evaporators' and cooling coils' inlets are connected to a supply source model representing the pumping well of the ATES. The flows of the source model are regulated by the climate controller and are assumed at 10°C (i.e. the ATES extraction temperature). Since the demand must be met at all times, the supply source has no flow restriction. Given an ATES target temperature of 15°C and 5°C, the models have been calibrated to ensure that the return temperature from the evaporator and the cooling coils is at $\pm 5\text{K}$ from the supply.

- **Simulation 2:** simulate the ATES model over the first year

Goal: compute the cold and warm plume formations and their status after the one year of injection.

In the first year, the ATES model is made of one extraction well and two injection wells. The injection flows and temperatures are imposed to the profiles computed in step one. For the cold well, these are the heat pump evaporator flows and return temperature. For the warm well, these are the cooling coils flows and their return temperature. The extraction flow is equivalent to the addition of the latter.

- **Simulation 3:** simulate the ATES model over the second year

Goal: compute the temperature evolution of the warm and cold wells over the year as a function of extracted volume.

In the second year, the ATES model is made of two extraction wells and one injection well. The model initialization conditions are set to the status at the end of one year of injection (i.e. the simulation from step two). Given that the greenhouse is assumed to have the same consumption, the same flow profiles are used. Over the second year, these are not injection but extraction flows: the cooling coils flows are the cold well extraction, the heat pump evaporator flows are the warm well extraction. The extraction temperature profile evolves due to the storage level and the losses to the environment. The temperature profile as a function of the extracted volume is the main result of the simulation.

- **Simulation 4:** simulate the overground models over the second year

Goal: compute the greenhouse demand with a supply from the cold and warm wells. Assess the energy efficiency of the global system in the ex-post.

The interconnected overground models are simulated for one year. The evaporator and cooling coils inlets are connected to two supply source models representing the warm and cold wells of the ATES. The temperature of the sources evolve as a function of the extracted volume given the results from step three.

5. RESULTS AND DISCUSSION

The main results of the overground models simulations (i.e. simulations 1 and 4) are summarized in Table 3. As it can be observed, for both simulations the climate controller succeeds in maintaining the air temperature within one degree of difference from the set-point during 82-83% of the time. The air temperature is outside the acceptable temperature range for the crop less than 1% of the time. This can be seen in Figure 4, which displays quarter-hourly data of the air temperature as a function of the set-point together with the thresholds of acceptable temperatures defined by the crop. The colors indicate whether the greenhouse was being heated, cooled or none of the above. It is observable that most of the points outside a 2 degrees range from the set-point value are on the upper side. This is because as explained in Section 3.3, the cooling system is not sized to supply the peak cooling demand but to respect the maximum acceptable threshold.

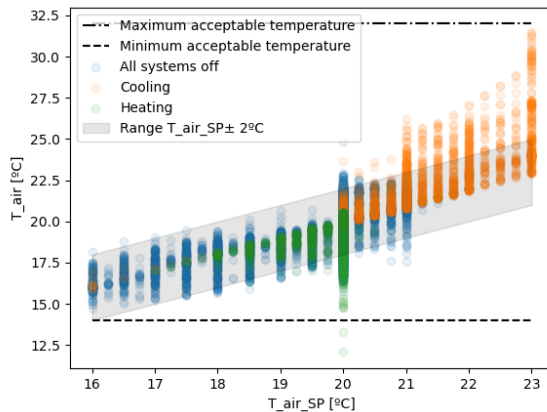


Figure 4: Comparison of the air temperature with respect to its set-point (quarter-hourly data points of simulation 1)

During the first simulation year, the greenhouse recovers 2338 MWh at the evaporator and 1546 MWh at the cooling coils. The accumulated volumes used in these exchangers are 403 dam³ and 398 dam³, respectively. The evolution of the accumulated volumes over the year is shown in Figure 5 (blue curves). The maximum extraction volumetric flow rate, which used to size the ATES, is 180 m³ h⁻¹. The return temperatures of the heat pumps and coils circuits are well controlled at ± 5 degrees with respect to the supply. After one year of simulation (Simulation 2), the warm and cold wells temperature is stable at 14.5°C and 5.7°C, respectively.

In Simulation 3, the recovered temperatures over a year as a function of the extraction volumes are obtained (Figure 5, red curves). As a reminder, Simulation 3 assumes that the greenhouse has the same demand profile as Simulation 1. As expected, the amount of energy stored decreases proportionally to the increase in extraction. In the warm well, the recovered temperature decreases over the year by a linear trend that follows the more or less linear demand profile. In the cold well, on the contrary, the absence of cooling demand at the beginning of the year allows for the temperature to be impacted by diffusion losses to the underground

flows. When the cooling demand becomes stable throughout summer, the recovered temperature increases in a linear fashion.

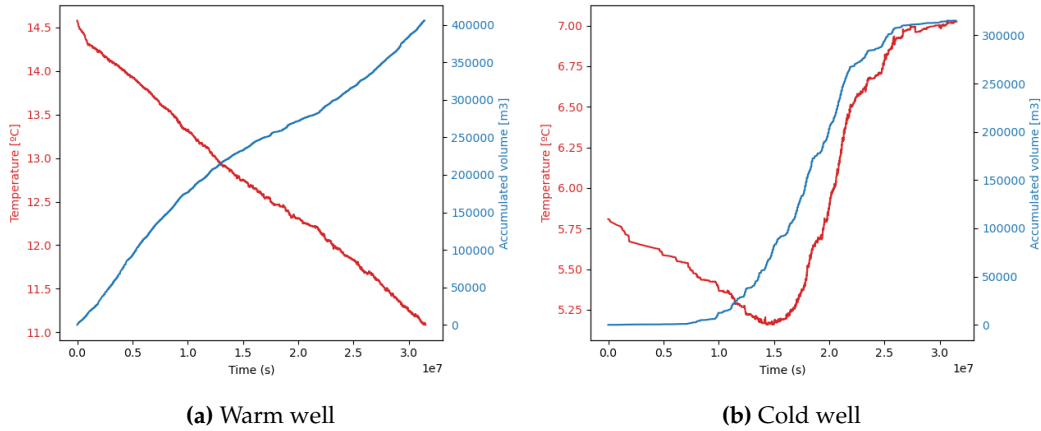


Figure 5: Evolution of the recovered temperature at the wells over one extraction year

In Simulation 4, the second simulation year in which the greenhouse demand is produced by the warm and cold wells (assumed at the temperature profiles from Simulation 3), the greenhouse recovers 3127 MWh at the evaporator and 1599 MWh at the cooling coils. On the one hand, and as expected since the climate set-points remain unchanged, these values are very similar to the ones from Simulation 1. On the other hand, given that the supply temperatures at the evaporator and the cooling coils are different, the required volumes for producing a heating or cooling capacity differ from the ones considered in Simulation 1. The volumes consumed at the evaporator and the cooling coils are now 437 dam³ and 216 dam³, respectively. This means that the heat volume consumed from the warm well in the second year (437 dam³) is higher than the volume stored in the first year (308 dam³). Similarly, the cooling volume consumed from the cold well in the second year (216 dam³) is lower than the volume stored in the first year (403 dam³). Over the years, this may lead to a system imbalance, mainly in the cold well side, since more energy is stored than consumed.

A way to avoid this imbalance is through the flexibility offered by greenhouses. Among the available measures that would help balancing the system, the ones that generate the most impact are:

- i) Reducing ventilation for temperature control: The greenhouse climate controller of Simulations 1 and 4 is programmed to use natural ventilation to cool the greenhouse when the outside temperature is lower than the targetted set-point. The greenhouse cooling consumption could therefore be increased by not opening the vents and using active cooling instead.
- ii) Decreasing the air temperature set-point to reduce heating in winter: As previously mentioned in this work, extreme temperatures are not optimal for crop yield and must be avoided. However, there is a range of near-optimal temperatures that allow for similar values of crop production rate. For instance, the harvest rate at a mean temperature of 14°C is 18% of the harvest rate at a mean temperature of 22°C. At the same time, the harvest rate at a mean temperature of 18°C is 87% of the one at 22°C (Vanhoor, 2011).
- iii) Increasing the air relative humidity ventilation threshold: natural ventilation is used when the air relative humidity increases above a threshold mainly to reduce the risk of crop diseases. Higher levels of humidity do not necessarily imply that the crop is affected by diseases, but because the risk on such diseases increases as humidity becomes higher, growers try to avoid such high moisture contents.

In order to illustrate the impact of these measures, Simulation 4 has been repeated twice producing variants 4b and 4c. The first, Simulation 4b, applies all three methods in the following fashion. The ventilation threshold for temperature control is increased from 1.5 to 2 degrees when heating is used, and from 1 to 2 degrees when no heating is used (i). The temperature set-point is modified in such way that the

average temperature set-point is decreased by 2 degrees with respect to the original simulation, but the lowest temperature set-point remains unchanged (ii). The threshold of ventilation for humidity control is increased from 85% to 90% from sunset until midnight (iii). The second, Simulation 4c, applies measures (ii) and (iii), and forbids ventilation for temperature control. That means, the vents can only open for humidity control. Measures (ii) and (iii) are applied as in Simulation 4b.

The obtained results, displayed in Table 3 and Figure 6, indicate that the measures can have a substantial impact on the greenhouse energy consumption. The modified set-points (measures ii and iii) decrease the heating needs down to 2502 MWh and increase the cooling demand up to 1995 MWh. In other words, measures (ii) and (iii) allow for increasing the cold well extraction by 40% (304 dam^3) and decreasing the warm well extraction by 29% (311 dam^3). A reduction on the ventilation for temperature control (measure i) as an additional measure allows for increasing the cold well extraction by 72% (371 dam^3) and decreasing the warm well extraction by 45% (241 dam^3), with respect to Simulation 4. Therefore, both methods decrease the system imbalance considerably, with measure (i) being the one with the most impact. However, as shown in Figure 7, when using measure (i) (Simulation 4c) the air relative humidity is above 90% during long periods, amounting for 30% of the year. The higher risk of diseases, although not quantifiable by the model, must be kept in mind and considered a drawback of this type of measure. In Simulation 4c, the integrated cooling rate (2561 MWh) is higher than the integrated heating rate (2012 MWh). This implies that, even in the Atlantic climate, the greenhouse can become a major cooling consumer.

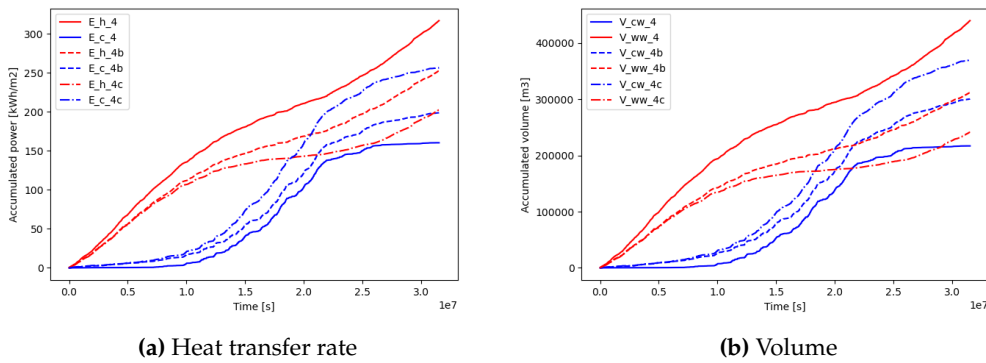


Figure 6: Accumulated heat transfer rate and volumes for simulations 4 and 4b

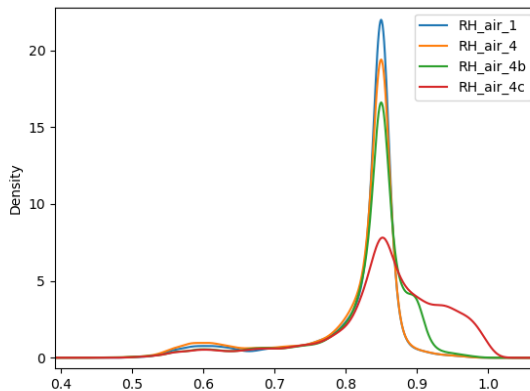


Figure 7: Density distribution of the air relative humidity over one year

Table 3: Simulation results

Variable	Unit	Sim 1	Sim 4	Sim 4b	Sim 4c
Simulation year	-	First	Second	Second	Second
Time T_air is within T_air_sp ± 1°C	%	82.12	83.70	84.57	86.84
Time T_air is within [14, 32]°C	%	100	100	99.40	99.45
Time RH_air is below 90 %	%	98.27	98.32	94.11	70.38
Average air temperature	%	20.04	20.02	18.36	18.39
Average air relative humidity	%	81.59	80.85	82.72	85.29
E_heat_total	MWh	2885	3127	2502	2012
E_heat_pipes	MWh	2117	2236	1979	1630
E_heat_coils	MWh	768.2	891.3	523.2	381.8
E_cool_total	MWh	1546	1599	1995	2561
E_el_total	MWh	3341	2802	2674	2589
E_el_lamps	MWh	2809	2265	2267	2272
E_el_hp	MWh	532.6	536.5	406.9	316.8
E_ev	MWh	2338	2595	2068	1661
V_ev	dam ³	403.3	436.9	310.8	241.6
V_cc	dam ³	307.8	216.4	304.1	371.3
V_ww	dam ³	307.8	436.9	310.8	241.6
V_cw	dam ³	403.3	216.4	304.1	371.3
Direction	-	Injection	Extraction	Extraction	Extraction
V_pw	dam ³	711.1	653.3	614.9	612.9
Direction	-	Extraction	Injection	Injection	Injection

6. CONCLUSIONS

In this work, the use of the thermal energy storage in shallow alluvial aquifers is proposed as a sustainable solution for supplying the energy demand of greenhouses. Air-conditioning greenhouses in summer allows for storing their energy surplus in an underground seasonal buffer that can later be used, in winter, for heating via a heat pump. The evaluation of the benefits arising from using ATES for supplying the energy demand in greenhouse applications requires the modeling of a greenhouse climate model, heating/cooling distribution and emission systems (i.e. heating pipes and coils), a heat pump and the ATES system. The models have been sized to the presented case study, which is based on a 100 m thick aquifer in the Cretaceous chalk, located in Wallonia (Belgium).

The case study has been simulated for two years. Due to the nature of the models, the experimental protocol is iterative and consists of 4 simulations. Results show that the recovered energy and volumes for heating and cooling are not in equilibrium. Greenhouses located in the Belgian latitude can be primarily considered as consumers of heating energy. Although energy is recovered during 3 months per year from cooling the greenhouse, the total energy consumed for heating is much higher. This results in a system imbalance on the cold well, since more energy is stored than consumed.

Despite this fact, a sustainable system can be achieved if the greenhouse climate controller is correctly calibrated. On the one hand, the great potential of flexibility offered by greenhouses allowed for improving the results in two extra simulations in which the greenhouse is forced to increase its cooling consumption. On the other hand, we observed a higher risk for crop diseases since a reduction of the ventilation to the outside air lead to a higher moisture content in the greenhouse. Not authorizing the opening of the vents for temperature control is therefore not desirable unless the greenhouse is equipped with a dehumidifier.

At this stage, the coupling between the two models (the aquifer and greenhouse ones) is not perfect. The results of one model are simply injected as inputs into the second and vice versa. This prevents us from going beyond the second year or simulating more complex (but probably more efficient) strategies. Therefore, a more tight coupling between the two models would be the natural continuation of this work for tackling optimisation strategies that lead to a sustainable, self-sufficient system.

NOMENCLATURE

α	polynomial coefficient	(–)
β	polynomial coefficient	(–)
δ	polynomial coefficient	(–)
ε	efficiency	(–)
ρ	density	(kg m ⁻³)
A	surface	(m ²)
c	specific heat capacity	(J kg ⁻¹ K ⁻¹)
COP	coefficient of performance	(–)
E	accumulated energy	(MWh)
EER	energy efficiency ratio	(–)
h	specific enthalpy	(J kg ⁻¹)
\dot{H}	heat flow associated to a mass transfer	(W)
\dot{M}	mass flow	(kg s ⁻¹)
\dot{Q}	heat flow	(W)
\dot{q}	specific heat flow	(W m ⁻²)
RH	relative humidity	(–)
T	temperature	(°C)
t	time	(s)
V	volume	(dam ³)
\dot{W}	electrical power	(W)
w	absolute humidity	(kg kg ⁻¹)

Subscript

air	air
c	contact
cc	cooling coils
cd	condenser
cool	cooling
cw	cold well
dry	dry
el	electricity
ev	evaporator
ex	exhaust
f	fictitious
fl	full-load
heat	heating
hp	heat pump
n	nominal
p	pressure
pl	part-load
pw	pumping well
su	supply
sens	sensible heat
sp	set-point
total	total
w	water
wb	wet-bulb
wet	wet
ww	warm well

REFERENCES

- Altes-Buch, Q. and V. Lemort (Dec. 2018). "Modeling framework for the simulation and control of greenhouse climate". In: *Proceedings of the 10th International Conference on System Simulation in Buildings*. Liege.
- Altes-Buch, Q., S. Quoilin, and V. Lemort (May 2022). "A modeling framework for the integration of electrical and thermal energy systems in greenhouses". en. In: *Building Simulation* 15.5, pp. 779–797. ISSN: 1996-8744. DOI: 10.1007/s12273-021-0851-2.
- Altes-Buch, Queralt, Sylvain Quoilin, and Vincent Lemort (Mar. 2019). "Greenhouses: A Modelica Library for the Simulation of Greenhouse Climate and Energy Systems". English. In: DOI: 10.3384/ecp19157533.
- Bloemendaal, Martin, Marc Jaxa-Rozen, and Theo Olsthoorn (Apr. 2018). "Methods for planning of ATES systems". en. In: *Applied Energy* 216, pp. 534–557. ISSN: 0306-2619. DOI: 10.1016/j.apenergy.2018.02.068.
- Bloemendaal, Martin, Theo Olsthoorn, and Frank Boons (Mar. 2014). "How to achieve optimal and sustainable use of the subsurface for Aquifer Thermal Energy Storage". en. In: *Energy Policy* 66, pp. 104–114. ISSN: 0301-4215. DOI: 10.1016/j.enpol.2013.11.034.
- Bolther, A. et al. (1999). *Méthode de calcul des consommations d'énergie des bâtiments climatisés ConsoClim*. Tech. rep. CSTB ENEA/CVA-99.176R. Paris: Ecole des Mines.
- Brandemuehl, Michael J. (1993). *HVAC 2 Toolkit: A Toolkit for Secondary HVAC System Energy Calculations*. en. Google-Books-ID: Bq7fAAAACAAJ. ASHRAE. ISBN: 978-0-910110-98-3.
- Commission, European (2021). *The tomato market in the EU: Vol. 3a: Trade for fresh products*. Tech. rep. AGRI.G2 - F&V - 2021, p. 29.
- De Schepper, Guillaume et al. (May 2019). "Assessment of short-term aquifer thermal energy storage for demand-side management perspectives: Experimental and numerical developments". en. In: *Applied Energy* 242, pp. 534–546. ISSN: 0306-2619. DOI: 10.1016/j.apenergy.2019.03.103.
- De Zwart, H.F. (1996). "Analyzing energy-saving options in greenhouse cultivation using a simulation model". PhD Thesis. Wageningen University.
- Gang, Wang, Liu Mingsheng, and David E. Claridge (Aug. 2007). "Decoupled modeling of chilled-water cooling coils". English (US). In: *ASHRAE Transactions*. Vol. 113 PART 1. ISSN: 0001-2505 Journal Abbreviation: 2018 ASHRAE Annual Conference. ASHRAE, pp. 484–493.
- Gendebien, Samuel, Stephane Bertagnolio, and Vincent Lemort (2010). "Comparative and empirical validation of three water cooling coil models". en. In: p. 8.
- Grisey, A. and E. Brajeul (2007). *Serres chauffées: réduire ses dépenses énergétiques*. 1st. Editions Centre technique interprofessionnel des fruits et légumes (CTIFL).
- Harbaugh, A.W. et al. (Jan. 2000). "MODFLOW-2000, the U.S. geological survey modular ground-water flow model-User guide to modularization concepts and the ground-water flow process". In: *U.S. Geological Survey Open-File Report 00-92*.
- Hecht-Méndez, Jozsef et al. (2010). "Evaluating MT3DMS for Heat Transport Simulation of Closed Geothermal Systems". en. In: *Groundwater* 48.5, pp. 741–756. ISSN: 1745-6584. DOI: 10.1111/j.1745-6584.2010.00678.x.
- Lebrun, J. et al. (1990). "Cooling Coil Models to be used in Transient and/or Wet Regimes". In: *Proceedings of the International Conference on System Simulation in Buildings 1990*, pp. 405–411.
- Morisot, O., D. Marchio, and P. Stabat (Apr. 2002). "Simplified Model for the Operation of Chilled Water Cooling Coils Under Nonnominal Conditions". In: *HVAC&R Research* 8.2. Publisher: Taylor & Francis, pp. 135–158. ISSN: 1078-9669. DOI: 10.1080/10789669.2002.10391433.
- Quoilin, S. et al. (2014). "ThermoCycle: A Modelica library for the simulation of thermodynamic systems". en. In: *Proceedings of the 10th International Modelica Conference*.
- Stanghellini, Cecilia, Bert Van 't Ooster, and Ep Heuvelink (Sept. 2018). *Greenhouse horticulture*. Wageningen Academic Publishers. ISBN: 978-90-8686-329-7. DOI: 10.3920/978-90-8686-879-7.
- Urban, L. and I. Urban (2010). *La production sous serre: La gestion du climat*. French. 2nd. Vol. 1. Lavoisier.
- Vanthoor, B. H. E. (2011). "A model-based greenhouse design method". dut. PhD Thesis. Wageningen University.
- Zheng, Chunmiao and Pu Wang (Jan. 1999). "MT3DMS: A Modular Three-Dimensional Multispecies Transport Model for Simulation of Advection, Dispersion, and Chemical Reactions of Contaminants in Groundwater Systems; Documentation and User's Guide". In:

ACKNOWLEDGMENT

The authors would like to thank the Walloon Region of Belgium for funding this research in the context of the EcoSystemePass project (convention 1510610).